Available online at www.sciencedirect.com

SciVerse ScienceDirect

Ceramics International 39 (2013) 1835–1840

CERAMICS INTERNATIONAL

www.elsevier.com/locate/ceramint

# Effect of the preparation route on the mechanical properties of Yttria–Ceria doped Tetragonal Zirconia/Alumina composites

S.M. Naga[a,*], E.M. Abdelbary[b], M. Awaad[a], Y.I. El-Shaer[b], H.S. Abd-Elwahab[a]

[a]*National Research Center, Ceramics Department, Tahrir street, Cairo, Egypt*
[b]*MTC, Engineering Mechanics, Cairo, Egypt*

Received 26 July 2012; received in revised form 9 August 2012; accepted 10 August 2012
Available online 1 September 2012

**Abstract**

Yttria–ceria doped tetragonal zirconia (Y, Ce–TZP)/ alumina ($Al_2O_3$) composites were fabricated by cold isostatic pressing at 350 MPa and firing at 1500 °C up to 1650 °C in air. Y, Ce–TZP/$Al_2O_3$ composite powders were prepared using two routes: (1) sol–gel method and in situ preparation of the composites, (2) mechanical mixing of as received μm powders.

In the present study, the role of the starting materials grain size on final density, microstructural development and mechanical properties of Y, Ce-TZP/$Al_2O_3$ composites were investigated. It was found that the ceramic bodies preparation route has a strong effect on the sintering behavior and mechanical properties of the final product.


*Keywords:* B. Microstructure; C. Mechanical properties; Y, Ce-TZP/$Al_2O_3$ composites

## 1. Introduction

Maiti and Sil [1] reported the effect of rare earth dopants $Yb^{3+}$, $Er^{3+}$ and $La^{3+}$ on the improvement of room temperature mechanical properties of $Al_2O_3$. They showed that the tendency for the growth of anisotropic elongated alumina grains resulted from the preferential segregation of the rare earth ions on basal planes (0 0 0 1) in alumina grain boundaries facilitates the improvement in toughness.

Rani et al. [2] showed that the addition of $Al_2O_3$ into $CeO_2$ and $Y_2O_3$ co-doped tetragonal zirconia depresses the grain growth of zirconia during sintering and improves the thermal stability of tetragonal zirconia in moist atmosphere, but degrades the sinterability.

Yin et al. [3] fabricated yttria–ceria doped tetragonal zirconia by hot isostatic pressing at 1400–1600 °C and 147 MPa for 30 min in Ar gas. They reported that the dispersion of $Al_2O_3$ into (Y, Ce)-TZP is useful to suppress the phase transformation from the tetragonal to the monoclinic structure during hot isostatic pressing. The fracture toughness and hardness were increased and the grain growth of zirconia was suppressed by the increase of $Al_2O_3$ content.

In the present work an attempt has been made to investigate the influence of the preparation route of isostatically pressed Y–Ce doped zirconia toughened alumina (ZTA) composites on the microstructural characteristics, physical and mechanical properties of the sintered composites.

## 2. Materials and methods

### 2.1. Mechanically mixed route

A composition of 85 wt% $Al_2O_3$, 10 wt% Y-PSZ and 5 wt% $CeO_2$ was made by powder mixing. The used aluminum oxide was of purity of 99.98% (provided by Almatis Gmbh Ludwigshafen/RH, Germany), while 5 mol% Y-PSZ was prepared by hydrolysis of zirconium (IV)-n-butoxide (Stream chemicals USA) with the addition of Yttrium nitrate ($Y_2O_3$ in $HNO_3$). The prepared gel was dried and calcined at 700 °C to get rid of all organic and nitrate materials. The calcined powder was ground to less than 10 μm and cerium (IV) oxide 99.5% min (RED) from

*Corresponding author. Tel.: +20 122174737.
*E-mail address:* salmanaga@yahoo.com (S.M. Naga).

0272-8842/$ - see front matter © 2012 Elsevier Ltd and Techna Group S.r.l. All rights reserved.
http://dx.doi.org/10.1016/j.ceramint.2012.08.031

Alfa Aesar UK. All powders were mechanically mixed using a ball mill for 5 h using 5 mm zirconia balls and polypropylene container with a constant speed of 300 rpm.

### 2.2. Sol–gel technique

The same composition was made by chemical technique of the precursors of alumina, zirconia and ceria using sol–gel technique. Aluminum tri-isopropoxide was hydrolyzed in distilled water and peptized by nitric acid. 5 mol% Yttria-partially stabilized zirconia was separately made by the hydrolysis of zirconium (IV)-n-butoxide with the addition of Yttrium nitrate ($Y_2O_3$ in $HNO_3$). $Ce(NO_3)_4 \cdot 4H_2O$ (BIO BASIC INC, Canada) was added to the hydrolyzed zirconium and aluminum alkoxide mixtures. The mixture was carefully stirred and allowed to cool till gellation. The formed gel was dried, calcined at 700 °C and ground to 10 μm.

### 2.3. Processing

The powders obtained from both processing routes were formed by uniaxial pressing at 220 MPa followed by cold isostatic pressing at 350 MPa for 5 min. into discs of 13 mm—diameter and 4 mm—height (for physical and microstrucural characterization) and rectangular bars of dimensions of $6 \times 6 \times 60$ mm (for mechanical evaluation). The formed shapes were fired in an electric oven at 1500–1650 °C with 50 °C intervals and one hour soaking time. Heating and cooling were conducted using rates of 5 °C/min.

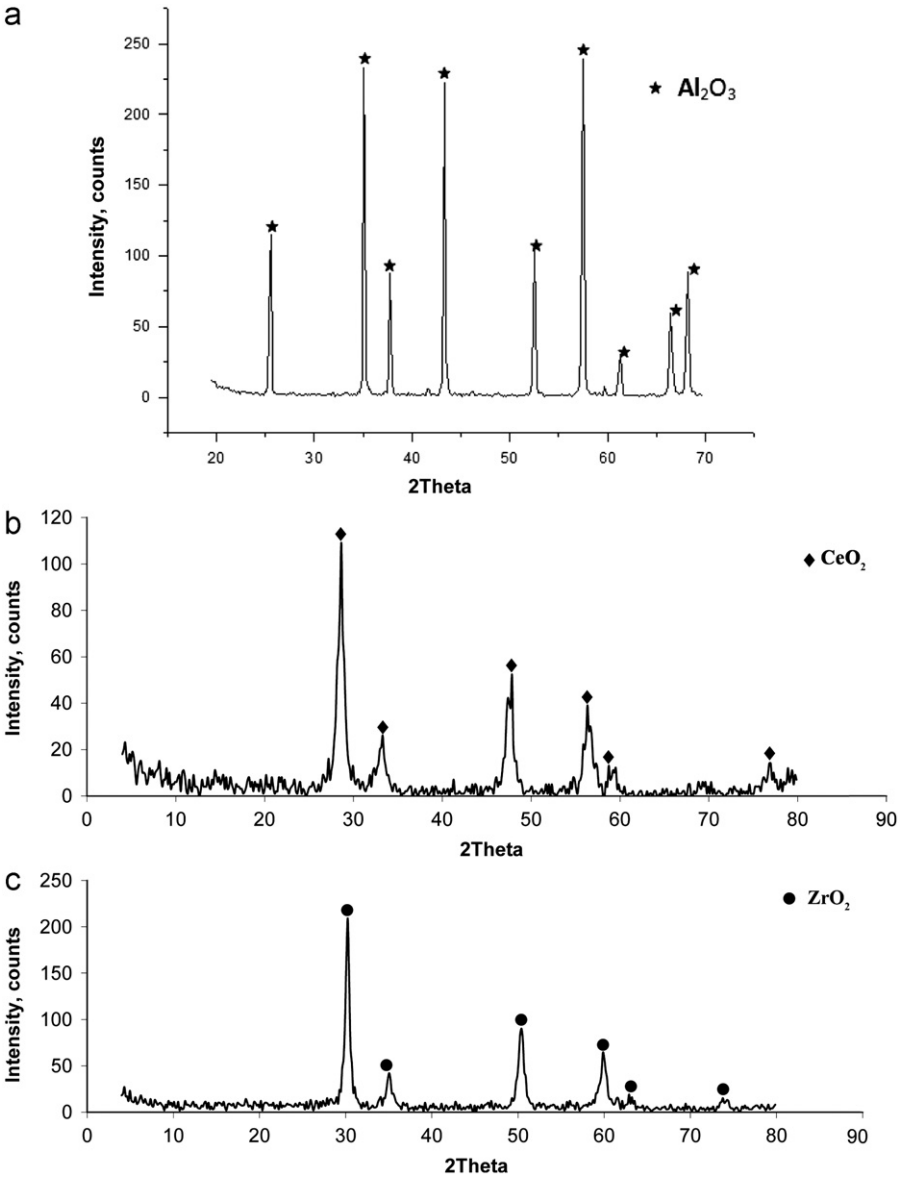


Fig. 1. XRD patterns of the starting materials, (a) Alumina, (b) Ceria and (c) Zirconia.

### 2.4. Characterization

The densification parameters of the fired samples in terms of bulk density and apparent porosity were evaluated by the liquid displacement method (ASTM C-20). The different phases developed during firing were identified by X-ray analysis (XRD) using a Philips X-ray diffractometer model PW: 1730 apparatus with a Cu target and Ni filter. Microstructure of the fracture etched surfaces was examined using scanning electron microscope (SEM-Jeol JSM-T20) apparatus coupled with an energy dispersion spectroscopy (EDS) equipment. Vickers hardness measurements were carried out for sintered samples by using micro hardness tester (Omnimet automatic MHK system Model Micro Met 5114, Buehler USA). Indentations were made on polished surfaces with a load of 1 kg held for 15 s. 30 indents were made for each sample and the average hardness was determined. Composite samples were polished down to 0.25 μm surface finish with diamond paste and thermally etched at 1000 °C for 1 h in air atmosphere. Bending strength was measured using a three point bending test on a universal testing machine (Model LLOYD LRX5K of capacity 5 KN) at a cross-head speed of 1 mm/min, and support distance of 25 mm. At least 10 specimens with the dimensions of 5 mm × 5 mm × 25 mm were measured for each data point.

## 3. Results and discussion

XRD analyses of the starting materials are shown in Fig. 1. All detectable diffraction peaks are corresponding to those of α-$Al_2O_3$ (Fig. 1a), cerium oxide (Fig. 1b) and tetragonal $ZrO_2$ (Fig. 1c). The effect of sintering temperature on the composites bulk density and apparent porosity are shown in Fig. 2. The figure clearly indicates that increasing the sintering temperature increases the bulk density of the composites and decreases their apparent porosity. On the other hand, the composites prepared via sol–gel route (S composite) show higher bulk density and lower apparent porosity in comparison to the composites prepared via mechanical mixing route (D composite).

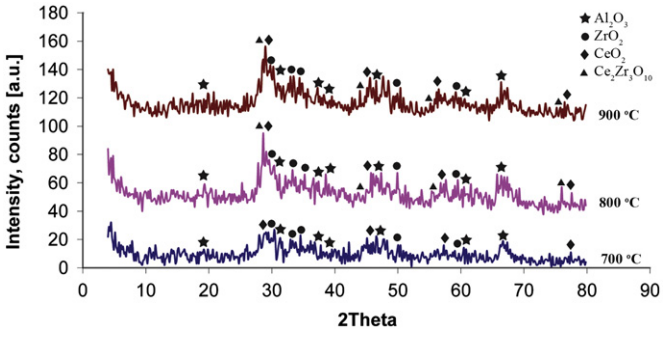


Fig. 3. X-ray pattern for S composite powder calcined at different temperatures.

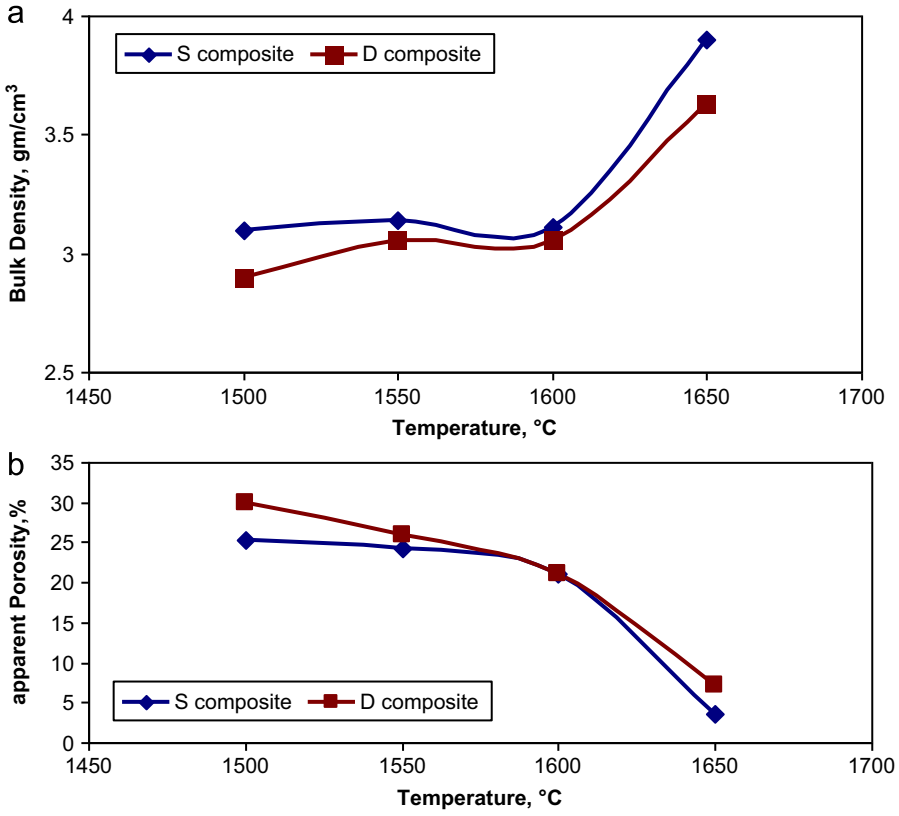


Fig. 2. Physical properties of the fired composites fired at different firing temperatures, (a) Bulk density and (b) Apparent porosity.

The improvement in the physical properties of S composite is due to the high degree of homogeneity achieved from the sol–gel technique. It is well known that sol–gel method is reliable because of its molecular level mixing and hence better homogeneity. It has the advantage of achieving perfect stoichiometry; thus leading to the desired shape and size distribution [4].

XRD pattern for the S composite samples calcined from 700 °C up to 900 °C in steps of 100 °C are shown in Fig. 3. X-ray pattern for samples calcined at 700 °C shows the

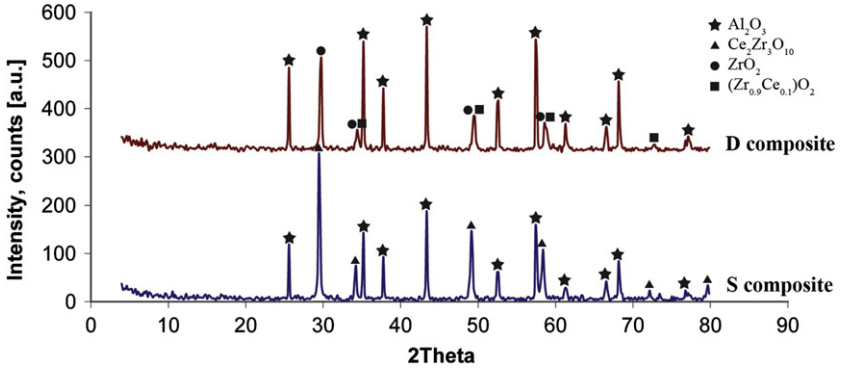


Fig. 4. X-ray pattern of the sintered S and D composites sintered at 1650 °C.

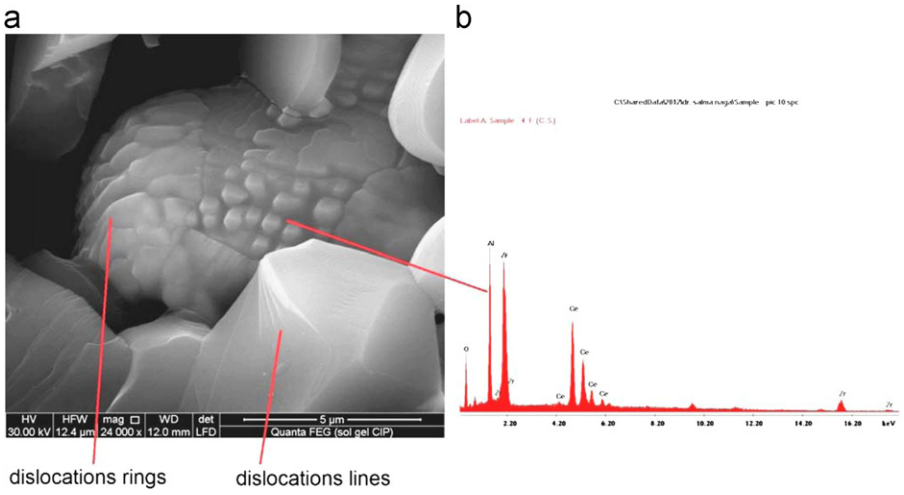


Fig. 5. (a) SEM micrograph of S composites Fired at 1650 °C and (b) EDS pattern.

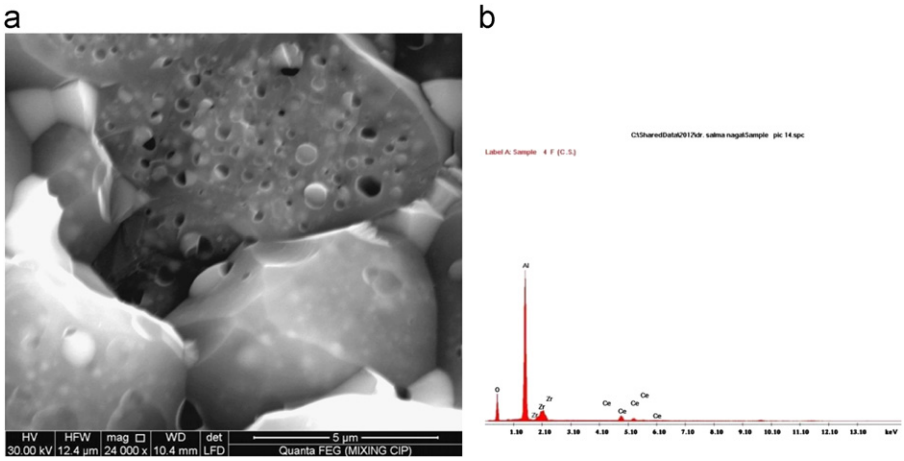


Fig. 6. (a) SEM micrograph of D composites Fired at 1650 °C and (b) EDS pattern.

presence of amorphous cerium oxide and the beginning of cerium–zircon oxide phase crystallization, whereas samples calcined at 800 °C are found to compose of tetragonal and orthorhombic zirconia together with $Al_2O_3$ crystalline phases. Further heating up to 900 °C is dominated by the tetragonal zirconia phase along with corundum and cerium–zircon oxide phases. Fig. 4 shows the XRD pattern of the sintered S and D composites sintered at 1650 °C. All the peaks in the pattern of S composite (Fig. 4a) belong to corundum and cerium–zircon oxide, while the pattern for D composite (Fig. 4b) consists of $Al_2O_3$, t-zirconia and cerium–zircon oxide. The absence of aluminum–cerium oxide phase indicates that there is no reaction between $Al_2O_3$ and $CeO_2$ under the used firing conditions.

Typical morphologies of dislocation in $Al_2O_3$/rare earth materials are found in S composite; Fig. 5a, where dislocation line and dislocation ring can be observed. On the other hand, D composite shows complex dislocations which are found inside the alumina grains near spontaneous microcrack; Fig. 6a. The forming mechanisms of these kinds of dislocation patterns are relatively complicated. The elastic strain energy can be deposited in the dislocations, which makes the dislocation in a sub-stable state. When the crack reaches the dislocations it can absorb parts of the energy of fracture through their own deformation. The propagating crack will be pinned and the fracture toughness of the material can then be increased [5]. Spherical particulate like crystals of cerium zirconate with grain size ranging between $\approx 0.11$ and 0.54 μm are found inside the alumina grains in addition to the main phase $Al_2O_3$ in the S composite; Fig. 5b. It was noticed that such grains are not observed inside the alumina grains of D composite, Fig. 6a. The microstructure of D composite fired at 1650 °C is given in Fig. 7. It consists broadly of two types of grain structures: small grains which have nearly round shape and larger grains possess irregular geometry including elongated shape. The small sized grains are $ZrO_2$ which situated at the intergranular and the triple junctions of the large grains; alumina grains. As the solid solubility of $ZrO_2$ in $Al_2O_3$ is low, $ZrO_2$ exists as a separate phase within the $Al_2O_3$ matrix. Fig. 8a shows the micrograph of S composite, in which the tiny bright particles of

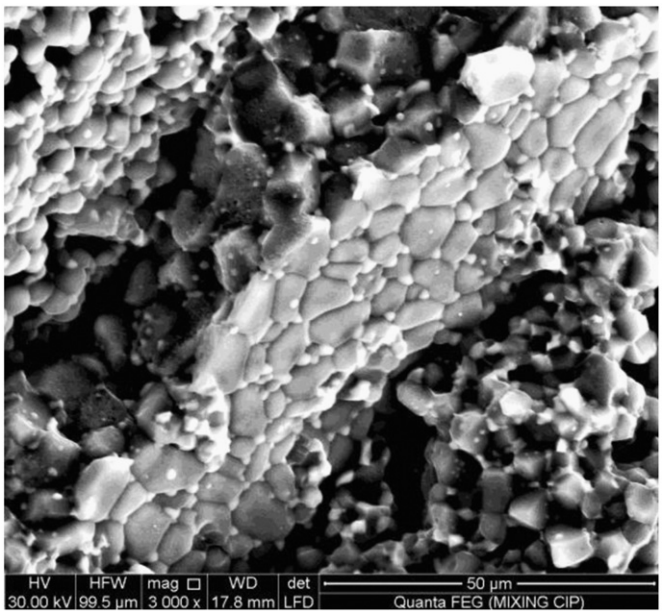


Fig. 7. SEM micrograph of D composites Fired at 1650 °C.

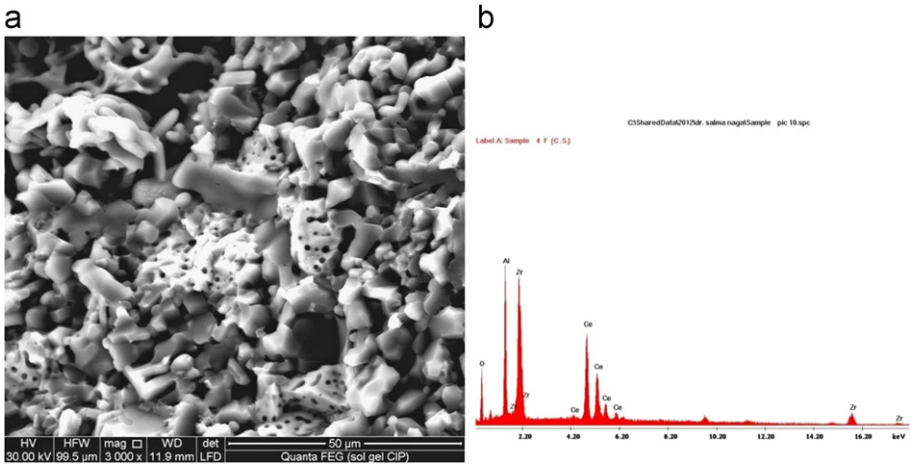


Fig. 8. (a) SEM micrograph of S composites fired at 1650 °C and (b) EDS pattern.

Table 1
Physical and mechanical properties of the fired composite.

| Sample symbol | Bulk density (g/cm$^3$) | Theoretical density (%) | Apparent porosity (%) | Vickers hardness, $H_v$ | Bending Strength (MPa) |
|---|---|---|---|---|---|
| S composite | 3.90 | 91.12 | 3.64 | 1385.47 | 219.79 |
| D composite | 3.62 | 84.81 | 7.17 | 1076.50 | 184.57 |

$ZrO_2$ are almost disappeared. EDS spectra obtained from the area analysis Fig. 8b shows the presence of cerium zirconate (the white porous grains) along with $Al_2O_3$ phase, which indicates that the preparation of yttria–ceria doped tetragonal zirconia/alumina composites via sol–gel route facilitates the entrance of $Ce^{3+}$ into $Zr^{4+}$ lattice to form cerium zirconate phase [6].

Vickers hardness and three point bending strength of S and D composite are shown in Table 1. The result indicates that both the Vickers hardness and bending strength of the sol–gel prepared samples (S composite) are higher than those of the mechanically mixed samples (D composite). Such behavior is attributed to the powder processing and the sinterability of the produced bodies. In contrast to D composite, zirconia powders used to fabricate S composite was obtained from the hydrolysis technique. As it was reported zirconia powders obtained from the hydrolysis technique have high sinterability [7]. The enhancement in strength of S composite is also, considered to be due to its microstructure which consisting of small grains with no large pores. The density of the S composite reached near the theoretical value rather than that of D composite.

## 4. Conclusions

1. The preparation route of S composite affected their physical properties. The improvement in the physical properties is due to the high degree of homogeneity achieved from the sol–gel technique used.
2. Mechanically mixed composites, D composite, show complex dislocations located inside the alumina grains.
3. The grain size of the cerium zirconate particles found in S composites fired at 1650 °C is ranging between $\approx 0.11$ and 0.54 μm.
4. Vickers hardness and bending strength of the sol–gel prepared composites, S composite, are higher than those of the mechanically mixed composites D composite.

## References

[1] K Maiti, A. Sil, Microstructural relationship with fracture toughness of doped and rare earth (Y, La) doped $Al_2O_3$–$ZrO_2$ ceramic composites, Ceramics International 37 (2011) 2411–2421.
[2] D.A Rani, Y. Yoshizawa, K. Hirao, Y. Yamauch, Effect of rare-earth dopants on mechanical properties of alumina, Journal of the American Ceramic Society 87 (27) (2004) 289–292.
[3] S. Yin, Y. Fujishiro, S Uchida, T. Sato, Characterization of ceria and Yttria co-doped zirconia/alumina composites crystallized in supercritical methanol, Journal of Supercritical Fluids 13 (1998) 363–368.
[4] M. Hirano, H. Inada, Fracture toughness, strength and Vickers hardness of Yttria–ceria-doped tetragonal zirconia/alumina composites fabricated by hot isostatic pressing, Journal Of Materials Science 27 (1992) 3511–3518.
[5] J. Judes, V. Kamaraj, Sol–gel preparation and characterization of ceria stabilized zirconia minispheres, Journal of Sol–Gel Science and Technology 49 (2009) 159–165.
[6] X. Chonghai, Study on microstructure of alumina based rare earth ceramic composite, Journal of Rare Earths 24 (2006) 217.
[7] Y. Murase, E. Kato, M. Hirano, Fabrication of dense, monoclinic $ZrO_2$ polycrystals by pressureless sintering, Yogyo Kyokaishi 91 (12) (1983) 562–564.